
Article:
Bardsley, K., Kwarciak, A., Freeman, C. et al. (3 more authors) (2017) Repair of bone defects in vivo using tissue engineered hypertrophic cartilage grafts produced from nasal chondrocytes. Biomaterials, 112. pp. 313-323. ISSN 0142-9612

https://doi.org/10.1016/j.biomaterials.2016.10.014

Repair of Bone Defects In Vivo using Tissue Engineered Hypertrophic Cartilage Grafts Produced from Nasal Chondrocytes

Katie Bardsley[1,3], Aga Kwarciak[2], Christine Freeman[1], Ian Brook[1], Paul Hatton, [1]Aileen Crawford[1*]

[1] School of Clinical Dentistry, University of Sheffield, 19 Claremont Crescent, Sheffield, South Yorkshire, S10 2TA. UK. [2] MRC Clinical Trials Unit at UCL, Institute of Clinical Trials & Methodology, Aviation House, 125 Kingsway, London, WC2B 6NH. UK. [3]Guy Hilton Research Centre, University of Keele, Staffordshire, ST4 7QB, UK.

*Correspondence Author

Dr Aileen Crawford,

School of Clinical Dentistry,

University of Sheffield,

19, Claremont Crescent,

Sheffield,

South Yorkshire,

S10 2TA.

UK

E-mail: a.crawford@sheffield.ac.uk

Phone: +44 1142 717939

Keywords: Bone tissue engineering, nasal chondrocytes, bone graft, hypertrophic cartilage, bone regeneration; maxillofacial reconstruction.

Abstract

The regeneration of large bone defects remains clinically challenging. The aim of our study was to use a rat model to use nasal chondrocytes to engineer a hypertrophic cartilage tissue which could be remodelled into bone in vivo by endochondral ossification.

Primary adult rat nasal chondrocytes were isolated from the nasal septum, the cell numbers expanded in monolayer culture and the cells cultured in vitro on polyglycolic acid scaffolds in chondrogenic medium for culture periods of 5-10 weeks. Hypertrophic differentiation was assessed by determining the temporal expression of key marker genes and proteins involved in hypertrophic cartilage formation. The temporal changes in the genes measured reflected the temporal changes observed in the growth plate. Collagen II gene expression increased 6 fold by day 7 and was then significantly downregulated from day 14 onwards. Conversely, collagen X gene expression was detectable by day 14 and increased 100-fold by day 35. The temporal increase in collagen X expression was mirrored by increases in alkaline phosphatase gene expression which also was detectable by day 14 with a 30-fold increase in gene expression by day 35. Histological and immunohistochemical analysis of the engineered constructs showed increased chondrocyte cell volume (31-45 µm), deposition of collagen X in the extracellular matrix and expression of alkaline phosphatase activity. However, no cartilage mineralisation was observed in in vitro culture of up to 10 weeks. On subcutaneous implantation of the hypertrophic engineered constructs, the grafts became vascularised, cartilage mineralisation occurred and loss of the proteoglycan in the matrix was observed. Implantation of the hypertrophic engineered constructs into a rat cranial defect resulted in angiogenesis, mineralisation and remodelling of the cartilage tissue into bone. Micro-CT analysis indicated that defects which received the engineered hypertrophic constructs showed 38.48% in bone volume compared to 7.01% in the control defects.

Development of tissue engineered hypertrophic cartilage to use as a bone graft substitute is exciting development in regenerative medicine. This is a proof of principal study demonstrating the potential of nasal chondrocytes to engineer hypertrophic cartilage which will remodel into bone on in vivo transplantation. This approach to making engineered hypertrophic cartilage grafts could form the basis of a new potential future clinical treatment for maxillofacial reconstruction.

1. Introduction

Bone is the second most transplanted tissue after blood. Despite this, the repair of large bone defects, whether congenital in nature or caused by trauma or disease remains clinically challenging. [1] Crucially, survival of transplanted bone tissue into a bone defect is dependent on the tissue receiving adequate blood supply to supply essential oxygen and nutrients and removal of waste products. Currently, autologous bone is the clinical 'gold standard' for bone tissue transplantation. Autologous bone is a living tissue with osteoconductive and osteoinductive properties which will not be rejected by the patient's immune system. There are, however, drawbacks to using autologous bone tissue including lasting post-operative pain from the donor site and donor site morbidity. [2] There are also limitations in the amount of healthy tissue that can be taken from a patient without causing instability in the remaining bone structures, an issue particularly pertinent in children. [2] Bone allografts and xenografts are used for bone repair, but these have to be decellularised to reduce their immunogenicity and as a consequence, are osteoconductive but have little osteoinductive capacity. Similarly, to date, current biomaterial bone graft substitutes have good osteoconductive properties but their osteoinductive properties are limited. Therefore, there is a strong clinical need to develop new bone graft materials for the repair and

regeneration of bone defects. Tissue engineering and regenerative medicine technologies are promising 'tools' to generate bone graft substitutes to fill this demand.

Most tissue engineering approaches have focussed on producing bone tissue by the route of intramembranous ossification in which mesenchymal stem cells are differentiated directly into osteoblastic cells to produce a bone-like extracellular matrix directly. One of the main challenges of bone tissue engineering by this route is the provision of a sufficient supply of nutrients and oxygen essential for the survival of the osteoblastic cells. During the culture of large three-dimensional tissue constructs, limited diffusion can cause problems in cell proliferation, differentiation and cell survival. Approaches to overcome these limitations include use of bioreactors [3,4] to provide dynamic culture conditions and engineering pre-vascularised grafts by including endothelial cells with differentiation signals to stimulate formation of blood capillaries [5].

Developmental tissue engineering, mimicking the natural pathways of tissue formation in body is a potential route to producing graft tissues for transplantation. Endochondral ossification is responsible for the formation of the axial skeleton and long bones [6] during embryogenesis and, is a potential and as of yet largely unexplored pathway of producing a suitable, alternative graft material for bone repair. Endochondral ossification involves the formation of a hypertrophic cartilage template which undergoes mineralisation, invasion by blood vessels and subsequent remodelling into bone. Hypertrophic cartilage formation and its remodelling into bone by endochondral ossification can be seen in the growth plate of young children and adolescents during periods of active growth and in the adult during healing of bone fractures where the 'soft' cartilage callus undergoes ossification into woven bone. In the growth plate, proliferative columnar chondrocytes produce a complex hyaline-cartilage extracellular matrix (ECM), in which the predominant protein is collagen type II. These

chondrocytes then undergo terminal differentiation to the hypertrophic chondrocyte phenotype and produce collagen type X in the ECM which is essential for mineralisation [7, 8].

Cartilage constructs have several advantages over the more extensively researched bone tissue constructs formed by intramembranous ossification. Cartilage can withstand lower oxygen concentrations than bone tissue containing osteoblasts and mesenchymal stem cells [9]. This advantage of cartilage allows for both the culture of larger grafts, as well as enabling better survival of the cartilage graft once implanted at the site of injury. Hypertrophic cartilage also contains the required biological factors to promote matrix remodelling [10], angiogenesis [11, 12], and bone formation [13], within the tissue. Therefore, once implanted in vivo, hypertrophic cartilage should recruit blood vessels and be remodelled into bone tissue via the normal physiological process of endochondral ossification. Hence, the potential of utilising tissue engineered hypertrophic cartilage warrants further research.

There has been widespread interest in the use of mesenchymal stem cells in regenerative medicine and tissue engineering for repair/regeneration of hyaline cartilage defects in the body; for example regeneration of articular cartilage in joints [14, 15] and cartilage defects in the head and neck area [16] for example, the nasal septum [17, 18]. In comparison, there has been little research focussed on engineering hypertrophic cartilage. Scotti et al demonstrated that bone marrow mesenchymal stem cells (BM-MSCs) in pellet culture were able to differentiate into hypertrophic-like chondrocytes which expressed both collagen type X and alkaline phosphatase and mineralised on subcutaneous implantation [7]. Scotti et al also reported that seeding BM-MSCs on a shaped collagen scaffold followed by chondrogenic priming formed a mineralised trabecular-like bone on subcutaneous implantation [19]. Sheehy et al [20] have also recently reported that BM-MSCs encapsulated in a shaped

hydrogel structure formed layer of mineralised tissue in the periphery of the constructs after in vitro chondrogenic priming followed by 8weeks of subcutaneous implantation. While mesenchymal stem cells have been approved for clinical use [21] other adult cells may offer an advantageous source for the production of a hypertrophic cartilage. Mesenchymal stem cells have been shown to produce cartilage with lower levels of ECM and reduced mechanical strengths when compared to adult chondrocytes [22, 23]. Primary adult hyaline chondrocytes, however, have been shown to produce high levels of GAG in the ECM when cultured in vitro, for the production of hyaline cartilage [22, 24].

In terms of using chondrocytes to form hypertrophic cartilage, previous research has shown that immortalised adult articular chondrocytes become hypertrophic and mineralised in pellet culture [25]. Also, immortalised chondrocytes derived human embryonic femurs were reported to produce osteoinductive signals in the culture medium [26]. There are, however, significant regulatory and safety concerns associated with the use of genetically modified cells for clinical applications. Two sources of adult chondrocytes, nasal septum and rib cartilage, have potential as sources of adult hyaline chondrocytes which can undergo terminal differentiation to the hypertrophic phenotype. Both tissues have capacity in vivo for the cartilage to undergo endochondral ossification; for example, where the nasal cartilage is attached to the facial bone. Also, both tissues can be harvested clinically by biopsy. The nasal septum is potentially a simpler biopsy procedure with a lower risk of donor site morbidity. In addition, chondrocytes extracted from the nasal septum have been broadly studied in tissue engineering for their capacity to produce a hyaline cartilage matrix [24, 27-29] and have been used clinically for repair of septal defects [17]. Only one detailed in vivo study to date has considered the use of nasal chondrocytes for tissue engineering a hypertrophic cartilage template for bone regeneration [30]. Here engineered constructs did not mineralise following

sub-cutaneous implantation, but were capable of some mineralisation following osteogenic pre-culture and implantation within ceramic scaffolds. More recently, a population of nasoseptal chondrocytes with progenitor features were described by Rotter and co-workers [31].

The overall aim of this study was to investigate whether chondrocytes isolated from the nasal septum, a potentially clinically relevant cell source, could produce a hypertrophic cartilage tissue which would remodel into bone on transplantation into a bone defect in vivo. Our first objective was to use a rat model in which to isolate and culture nasal chondrocytes and investigate whether the chondrocytes would produce a hypertrophic cartilage matrix in 3D culture using a poly-L-glycolic acid (PGA) scaffold support. Chondrocytes were also isolated from the rib and cultured in the same way as a comparator. The second objective was to implant the engineered hypertrophic cartilage subcutaneously in vivo to investigate biocompatibility, and angiogenesis in the implant. The engineered hypertrophic cartilage was also implanted in an in vivo bone defect in the calvaria of the rat to determine whether the cartilage would undergo remodelling into bone.

2. Materials and methods

2.1 Cell Isolation and Expansion

Nasal and rib cartilages were harvested from 6 week old Wistar rats within 2 hours of euthanasia and the chondrocytes isolated and cultured as we have described previously [32, 33] and is a similar method of cell isolation and expansion as reported by other researchers [24, 29, 31,] Briefly the cartilages were removed, washed in phosphate buffered saline (PBS) and any epithelial tissue removed by scraping the cartilage surfaces with a scalpel blade. The cartilages were again washed with PBS, cut into small pieces and incubated in 2.5% trypsin (Sigma Aldrich, UK) for 30 minutes followed by an overnight digestion in 3 $mg.ml^{-1}$ bacterial collagenase Sigma Aldrich, UK) in basic medium [Dulbecco's modified eagle medium (DMEM) (Sigma Aldrich, UK) supplemented with non-essential amino acids (NEAA) (Sigma Aldrich, UK), 100 $units.ml^{-1}$ penicillin and 100 $ug.ml^{-1}$ streptomycin (Sigma Aldrich, UK), and 10 mM HEPES buffer (Sigma Aldrich, UK) and 10 % foetal calf serum (FCS, Biosera, UK)]. The chondrocytes were isolated from the digested tissue by passing the digested tissue through a 70 µm cell strainer (BD Biosciences, UK) followed by centrifugation (10 min, 192g) to pellet the cells. The cell pellet was washed to remove by suspending the cells in PBS and repeating the centrifugation step. This washing step was repeated once more and the final cell pellet suspended in basic culture medium containing 10 $ng.ml^{-1}$ of fibroblast growth factor-2 (FGF-2, Peprotech, UK). The cells were plated into culture flasks and cultured in an incubator at $37^{o}C$ a humidified atmosphere of 5% CO_2 and 95% air. The culture media (basic medium containg10 $ng.ml^{-1}$ FGF-2) was changed twice per week.

2.2 Scaffold

A commercial PGA scaffold (Biofelt®, Cellon S.A., Luxembourg) was used. The Biofelt® scaffold was a biodegradable, 1 mm thick, non-woven PGA felt with a bulk density of 70mg.cc^{-1} and was fabricated from medical grade polymer. For experiments, 5 mm diameter discs were cut from the scaffold sheet using a cork borer and the discs were covered with isopropanol for 15 min. to sterilise them, a method recommended by the manufacturer. The isopropanol was removed and the discs washed extensively with sterile PBS to ensure removal of the isopropanol. The scaffold discs were then conditioned in basic media for a further 20 minutes. This scaffold has been reported extensively, primarily as a reference material in investigations of novel biomaterials [34-36].

2.3 Scaffold Seeding and 3D Culture

At passage 2, 2x10^6 cells were seeded per PGA scaffold for 72 hours in basic medium on an orbital shaker set at 35 revolutions per minute (rpm). The seeded constructs were removed and placed in fresh culture medium and then cultured for 42 days in basic medium containing 1 µg.ml^{-1} insulin and 50 µg.ml^{-1} ascorbic acid, to induce chondrocyte differentiation and extracellular matrix formation. After culture, the constructs were removed from the culture wells, lightly blotted with tissue to remove excess medium and weighed. The constructs were bisected perpendicularly and for each construct, one half was frozen at -20 ^{o}C for analysis of GAG content and the remaining half was mounted in Optimal Cutting Temperature (OCT) cyromountant and stored at -20 ^{o}C for histology and immunohistochemistry.

2.4 Glycosaminoglycan assay

Freeze dried constructs were digested overnight at 60 ^{o}C in 200 mM phosphate buffer, pH 6.8, containing 1 mM EDTA, 6 mM n-acetyl cysteine and 0.05 % (w/v) papain (from papaya

latex, Sigma Aldrich UK) After digestion, the samples were centrifuged at 10,000g to pellet remains of the PGA scaffold and the supernatant fraction was removed and stored at -20^{o}C until assay for glycosaminoglycan (GAG) content, The GAG concentration of the digested samples was determined using 1,9-dimethylmethylene blue (DMB) following the protocol described by Farndale et al. [37].

2.5 Histology

8 μm frozen sections were taken from OCT-mounted constructs and transferred to 3-aminopropyltriethoxysilane (APES) coated slides. Sections were fixed in paraformaldehyde and stained using Haematoxylin and Eosin (Sigma Aldrich, UK), to determine general tissue morphology. Sections were also stained for extracellular matrix GAGs using Alcian Blue [1 % (w/v) Alcian Blue in 3% acetic acid pH 2.5, (Sigma Aldrich, UK)] and counterstained with a 0.5 % (w/v) aqueous solution of Neutral Red (Sigma Aldrich, UK), or 1% (w/v) Toluidine Blue in 0.5 % (w/v) sodium borate, (Sigma Aldrich, UK). Mineral deposition was determined by staining construct sections with 1.4 % Alizarin Red aqueous solution pH 4.1, (Sigma Aldrich, UK). Distribution of alkaline phosphatase was assessed in the construct sections using SIGMAFAST^{TM} BCIP$^{®}$/NBT (5-bromo-4-chloro-3-indoyl phosphate/ Nitro blue tetrazolium, Sigma Aldrich, UK) according to the manufacturer's instructions.

2.6 Immunohistochemistry

Immunohistochemistry was used to assess collagen type II and X deposition throughout the constructs. Collagen expression was investigated using commercial antibodies: goat anti-collagen type II antibody (dilution 1:20 Cambridge Bioscience, UK) and mouse anti-collagen type X antibody (dilution 1:100, Quartet, Berlin, Germany). Detection was carried out with complementary secondary biotinylated antibodies (Vectastain ABC kit, Vector Laboratories

Ltd, UK) and visualization performed with diaminobenzidine tetra hydrochloride (DAB) substrate (Vector Laboratories Ltd, UK). The cell nuclei were counterstained with Mayer's Haematoxylin (Sigma Aldrich, UK). Supplementary Figure 1 shows in detail the low level of non-specific staining obtained using the antibodies. Images showing the level of non-specific staining in each experiment are shown as inserted images in the immunohistochemical images.

2.7 Real Time RT-PCR (q-PCR)

After culture, the constructs were washed in PBS and flash frozen in liquid nitrogen for 30 seconds. A tissue pulveriser was used for 1 minute to homogenise the sample in PBS and the samples centrifuged at 11,000 rpm for 2 minutes. RNA was extracted immediately from the tissue pellet using a Bioline Isolate II RNA Mini Kit (Bioline Reagents Ltd, UK) and the concentration determined using a Nanodrop 2000. cDNA was synthesised using a high capacity RNA to cDNA master mix (Life Technologies, UK) and 100 ng of RNA per reaction. Reactions were run in a thermal cycler using a cycle of 10 minutes at 25 °C, 2 hours at 37 °C, 5 minutes at 85 °C and then 10 minutes at 4 °C.

Real time PCR was performed using a 7900 Fast Real Time PCR machine in a 96-well plate with an experimental volume of 10 µl. Taqman probes and primers (Life Technologies, UK) were used for the detection of the expression of collagen type II, alpha 1 (Rn01637087_m1), collagen type X, alpha 1 (Rn01408030_m1), alkaline phosphatase (Rn00575319_g1), indian hedgehog (IHH) (Rn03810376_m1), SRY (sex determining region Y)-box 9 (Sox9) (Rn01751069_mH) and runt-related transcription factor 2 (Runx2) (Rn01512298_m1). Non template and reverse transcriptase negative controls were used to check for cDNA contamination.

Results were analysed using the ΔΔct method in relation to the housekeeping gene, glyceraldehyde 3-phosphate dehydrogenase (GAPDH) (4352338E) expression. The ΔΔct value was then normalised to undifferentiated 3D culture chondrocytes, to assess the differentiation on the PGA scaffold material.

2.8 In vivo Experiments

2.8.1. Subcutaneous implantation of constructs.

Rat nasal chondrocytes were cultured on PGA scaffolds under standard conditions as described above. The scaffolds were cultured in vitro for 42 days. This time period was used to enable the culture expanded cells to regain their chondrogenic phenotype and maximise expression of hypertrophic features (as indicated by the in vitro qPCR, histological and immunohistochemical data). At day 42 several PGA constructs were cryopreserved in OCT. This group formed the 6-week in vitro control to enable determination of the stage of chondrocyte differentiation prior to implantation. The remaining constructs were either implanted subcutaneously for 4 weeks (1 hypertrophic construct per animal plus 1 cell-free/empty scaffold control) or left for a further period of 4 weeks in in vitro culture to match the time period of the in vivo implantation. This latter group formed the 10-week in vitro control to investigate any further changes which would occur on extending the in vitro culture period for a further 4 weeks. All experiments were carried out under the appropriate Home Office regulatory licence (Licence number 40/2795). 12-week old Wistar rats (n=4) were kept under conventional housing conditions with free access to food and water. The constructs and empty scaffolds were placed in subcutaneous pockets on the backs of anaesthetised animals. After 4 weeks, the rats were sacrificed and the constructs retrieved. Cell-free/empty scaffolds could not be retrieved after 4 weeks of implantation as they had completely dissolved.

2.8.2. Insertion of constructs into a cranial defect in the rat.

Constructs were cultured in vitro for 35 days to enable the culture expanded cells to regain their chondrogenic phenotype and gain hypertrophic features after which, they were washed in PBS prior to implantation into the cranial bone defects. The constructs were placed in 4 mm full thickness healing defects in the calvaria of 8-week old Wistar rats. All in vivo experiments were performed under the appropriate Home Office animal license (license number: 40/3311).

Rats were anaesthetised using IsoFlo (Isofluorane, Abbott Laboratories, UK) and given antibiotics, Synulox (Pfizer, UK), and a painkiller, Metacam (Boehringer-Ingleheim, Germany). The anesthetised animals were weighed and a midline incision was made in the skin covering the skull and both the skin and periosteum were retracted to reveal the cranium. Two 4 mm full thickness defects were drilled into the skull using a 3.5 mm diamond burr with saline irrigation. The constructs Grafts were cut to 4 mm diameter using a sterile biopsy punch and placed into one of the defects with the other being left empty. The periosteum was closed over the defects and secured with 2 vicryl stitches, before the wound was closed using 4-5 stitches.

Constructs were left in the cranial defects for 4, 8 or 12 weeks, before the animals were culled. Rats were anesthetised using IsoFlo and their vertebrae separated, the heads were then removed from the animal and placed in 10 % (w/v) neutral buffered formalin. The cranial defects were then examined by microcomputed tomography (micro-CT) and histology to assess the degree of new bone formation in the defect area.

The skulls were analysed using a desktop high resolution micro-CT system (Skyscan 1172, Skyscan, Belgium). Scans were performed at 100 kVp, with a 1 mm aluminium filter and a

pixel size of 12.1 μm. Images were taken throughout 360 ° with 2 images being averaged at each point.

After micro-CT analysis the soft tissue was removed and the skulls decalcified by incubation in an aqueous solution of 0.5 M EDTA and 0.4 M sodium hydroxide in pH 7.0 for 14 days. After decalcification the craniums were dissected and embedded in paraffin wax for histological analysis.

3. Results

3.1 Analysis of Constructs

Sternal and nasal hyaline chondrocytes were compared for their ability to undergo hypertrophic differentiation on PGA scaffolds. Both sternal and nasal-derived chondrocytes seeded onto the scaffolds to a similar extent (over 90% seeding efficiency). The constructs were incubated for up to 42 days after which they were terminated and analysed as described in the methods. Deposition of proteoglycan, collagens II and X showed extensive distribution in constructs formed from either nasal or sternal chondrocytes by day 42 (Figure 1). An increase in cell volume was found in constructs from both chondrocyte types and collagen X deposition was observed in areas of chondrocytes showing increased cell volume. (Figure 1) Quantification of the ECM deposition was assessed by determining the amount of proteoglycan deposition by measuring the levels of GAGs (expressed as a percentage of the dry weight of the construct ECM). The percentage of GAGs increased in the ECM with the duration of culture and reached similar levels in constructs of nasal chondrocytes (28.75% ± 1.25) and sternal chondrocytes (30.0% ±1.25) by day 42. Alkaline phosphatase activity was widely distributed throughout constructs of nasal chondrocytes (Figure 1b, presence of

alkaline phosphatase activity shown by back/brown staining). In contrast, little alkaline phosphatase activity was detected in constructs from sternal chondrocytes (Figure 1a) indicating a full hypertrophic chondrocyte phenotype in the sternal chondrocytes was not achieved under the incubation conditions used. Therefore, constructs formed from nasal chondrocytes had the capacity to express features of hypertrophic chondrocytes and were used to further investigate the hypertrophic phenotype and determine whether they could be remodelled into bone tissue in vivo

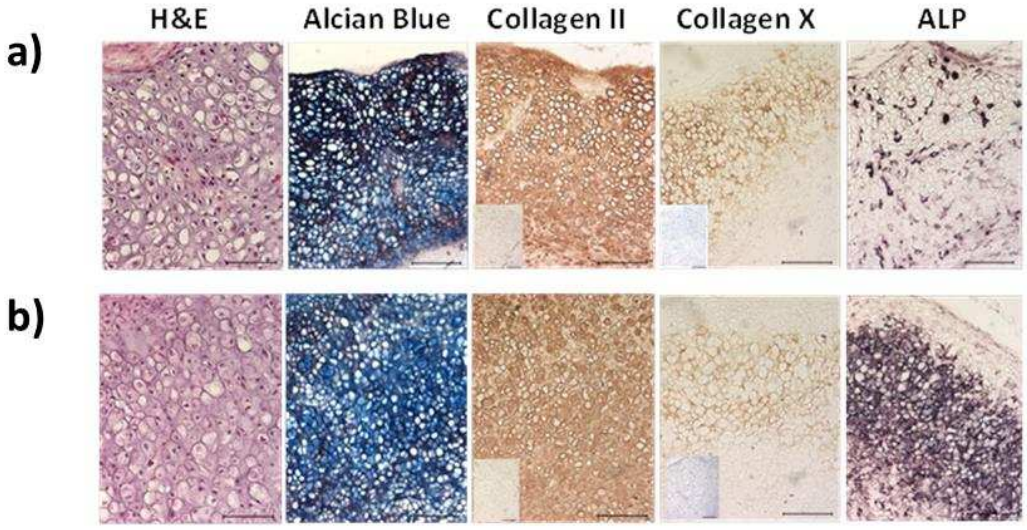

Figure 1: Representative histological and immunohistochemical staining of tissue sections of constructs of sternal (**a**) or nasal chondrocytes (**b**) seeded on PGA scaffolds and cultured for 42 days. The legend above the images show the staining procedures used. Images show histochemical staining by Haemotoxylin and Eosin (H&E) to show general tissue morphology, distribution of proteoglycan (shown by Alcian Blue staining, proteoglycans stained blue), localisation of collagen II and collagen X (collagen localisation shown by brown staining) and histochemical staining for alkaline phosphatase activity (ALP, enzyme

activity shown by black/brown stained). Control sections showing non-specific antibody staining are inserted into the immunohistochemical images. Scale bars = 200 µm.

Significant morphological and phenotypical changes were observed within constructs of nasal chondrocyte throughout the 42-day culture period (Figure 2a). After seeding of the constructs and during the early culture period, the nasal chondrocytes exhibited a cell size and morphology equivalent to that of a hyaline chondrocyte phenotype (8-12 µm, day 14). By day 28 of culture, chondrocytes with an increased cellular size (31-45 µm), indicative of a hypertrophic phenotype, were observed in isolated pockets of the constructs. By day 42 of culture, the constructs showed a uniform distribution of hypertrophic-like chondrocytes. Regarding extracellular matrix (ECM) formation, little deposition (in terms of collagen II and proteoglycan) was observed by day 14 in the constructs. However, the ECM deposition increased with the length of incubation as shown by the increasing tissue morphology at days 28 and 42 and localisation and increasing deposition of proteoglycans within the constructs, as shown by quantitative determination of GAGs (a measure of proteoglycan) in the constructs (Figure 2b). Expression of the major cartilage proteins within the ECM was also altered throughout the culture period and indicative of hypertrophic differentiation. The constructs showed expression of collagen type II by day 14 with no detectable expression of collagen type X. By day 28, collagen X was detected in the constructs in areas showing hypertrophic chondrocytes. However, little alkaline phosphatase activity was observed at this time point. By day 42, both collagen X and alkaline phosphatase localisation were observed along with most cells showing a hypertrophic morphology (Figure 2a). The degree of mineralisation of the construct was assessed at day 42 and while the constructs showed

hypertrophic differentiation in terms of alkaline phosphatase and collagen X protein deposition, no mineralisation was detected during the in vitro culture period.

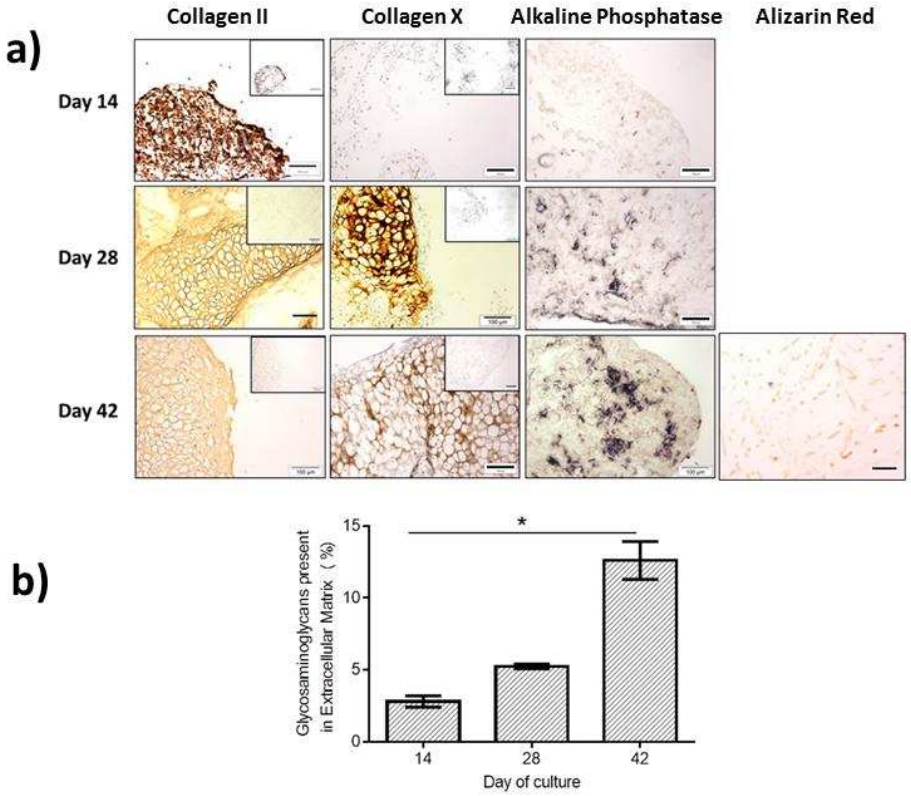

Figure 2: (**a**). Representative histological and immunohistochemical staining of tissue sections from nasal chondrocytes seeded on PGA scaffolds and cultured for 14, 28 and 42 days. The images show immunolocalisation of collagens II and X and alkaline phosphatase activity. Collagen II was detectable from day 14. By day 28, the chondrocytes exhibited an increased cell size and collagen X was detected with an extensive distribution of collagen X by day 42. Alkaline phosphatase activity was also detectable at days 28 and 42. Calcium deposition was investigated using Alizarin Red after 42 days of incubation; however, no calcium deposition was observed. (**b**). Shows the glycosaminoglycan (GAG) accumulation (expressed as a % of the tissue dry weight) in the nasal chondrocyte constructs with time of in vitro culture. During the 42 day culture period the amount of GAG in the constructs increased, indicating increased extracellular matrix deposition throughout the incubation

period. (n=6, errors plotted as standard error of the means, * $p<0.05$). Scale bars=100µm. Control sections showing non-specific antibody staining are inserted into the immunohistochemical images.

3.2 Effect of 3D Culture on Chondrocyte Gene Expression

After isolation from native cartilage, the nasal chondrocytes were grown in 2-dimensional (2D) monolayer culture to expand the numbers of cells. After culturing the chondrocytes on the PGA scaffold for 72 hours in basal media a distinct change in the gene expression was observed (Supplementary data, Figure 2) compared to the 2D monolayer cultures. Significant increases in the expression of Ihh, Sox9, and collagen type II were observed indicating the chondrocytes were reverting to a more hyaline phenotype. Conversely markers of hypertrophic differentiation, collagen type X, alkaline phosphatase and Runx2, were significantly decreased during the first 72h of culturing the chondrocytes were in the 3D environment of the PGA scaffolds.

3.3 Effect of Differentiation on Chondrocyte Gene Expression

Gene expression within the cartilage constructs changed significantly throughout the 42-day culture period following the scaffold seeding period (Figure 3). The ECM component, collagen II, a marker of a hyaline chondrocyte phenotype, continued to increase after the initial 72 hour cell- seeding period, until day 7 where a 6-fold increase in gene expression was observed. After day 7, the gene expression of collagen II was significantly downregulated throughout the remainder of the culture period (Figure 3a). Conversely, gene expression for collagen X increased from day 7 to day 14 with a reproducible decease in expression at day 21 followed by increase expression to reach a peak of 100-fold increase at

day 35 (Figure 3b). Similarly, gene expression for alkaline phosphatase increased from day 7 to peak levels by days 35 (Figure 3c). The gene expression of the signalling protein, Indian hedgehog (IHH), a pre-hypertrophic marker, rose from day 14 with a significant peak in expression by day 21 (30-fold increase) before falling to lower levels (6 fold) (Figure3d). Gene expression of the transcription factor Sox9 was significantly reduced at day 3 until day 35 when there was an increase in expression corresponding with the timing of peaks in collagen type X and alkaline phosphatase gene expression (Figure 3e). Expression of the transcription factor, Runx2 was increased by day 14 of the culture period and reached a peak in gene expression by day 28. Gene expression of Runx2 then deceased to around 3-fold increase at day 35 (Figure 3f).

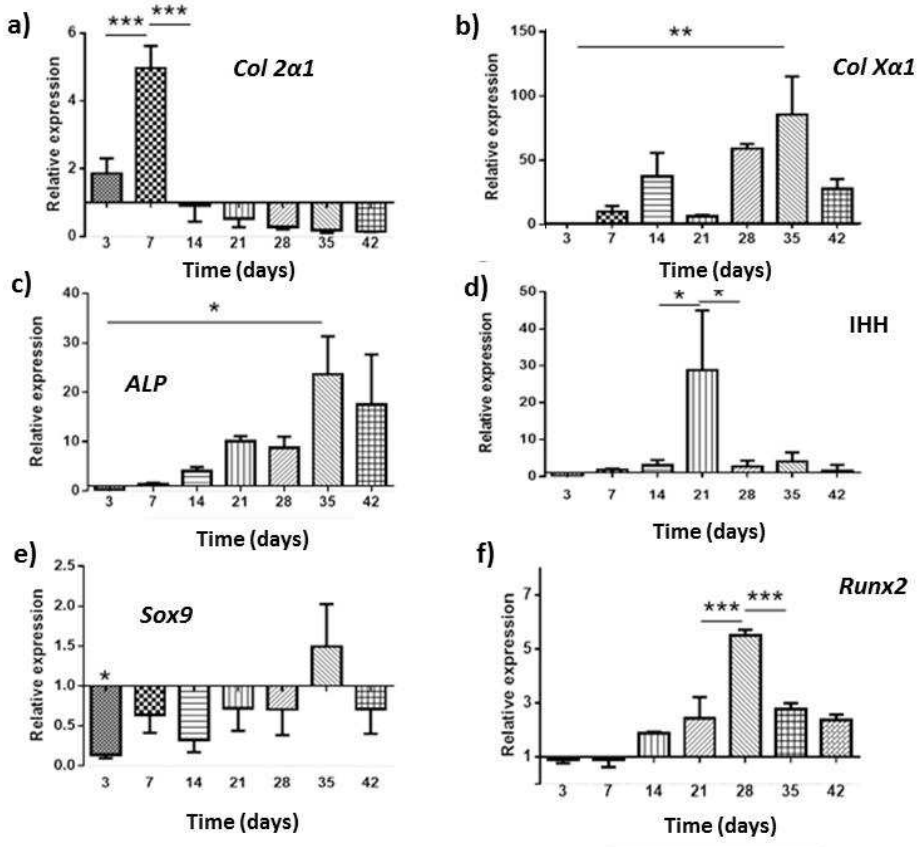

Figure 3: mRNA expression of genes associated with endochondral ossification during hypertrophic differentiation. Data was normalised to gene expression observed after the 72-hour period of cell seeding of the scaffold. **(a)** collagen type II (Col 2α1 chain); (**b**) collagen type X (Col Xα1 chain); **(c)** alkaline phosphatase; **(d)** Indian hedgehog (IHH); **(e)** SRY (sex determining region Y)-box 9 (SOX9) and (**f**) runt-related transcription factor 2 (Runx2). (* $p<0.05$)**,** ** $p<0.01$ and *** $p<0.001$. n = 4)

3.5 In Vivo Repair

Subcutaneous implantation

Since the hypertrophic constructs failed to mineralise in vitro; subcutaneous implantation of the hypertrophic constructs was carried out to determine if the constructs would undergo mineralisation in vivo. Before implantation, the constructs showed features of hypertrophic cartilage tissue shown by areas of hypertrophic cells; some areas of collagen X deposition in the ECM and alkaline phosphatase enzyme activity (refer to Supplementary Figure 3). Histological analysis of the retrieved constructs revealed that they were encapsulated by a thin layer of fibrous, connective tissue. Immunolocalisation studies, using anti-CD45+ to detect leukocytes and anti-CD68+ antibodies to detect macrophages, showed some inflammatory cells were present around the outer areas of the retrieved constructs but their localisation was sparse and was restricted mostly to non-cartilage areas (Supplementary Figure 4). No giant cells were detected.

Numerous blood vessels were present on the surface of implants and throughout their interior after 4 weeks of implantation (Figure 4b, g). Tissue remodelling was observed in regions adjacent to connective tissue in the periphery of the cartilage construct and around areas invaded with blood vessels (Figure 4g) cartilage matrix remodelling is clearly visible on

sections stained with Alcian Blue and Eosin where single chondrocytes, were still embedded in a thin layer of GAGs, are surrounded by newly formed non-cartilaginous matrix (Figure 4g). After 4 weeks of implantation collagen X was distributed throughout the cartilaginous areas of constructs (Figure 4a, b). Additionally, alkaline phosphatase was detected in the implanted constructs (Figure 4c, d). In contrast to the in vitro experiments, after 4 weeks of implantation calcium deposition was observed in all the samples (Figure 4e, f) Mineralised matrix was found in cartilaginous areas around the chondrocytes and it was largely co-localised with areas of high alkaline phosphatase activity. However histologically, the mineralisation appeared to be due to mineralised cartilage as no apparent bone formation was observed in these experiments.

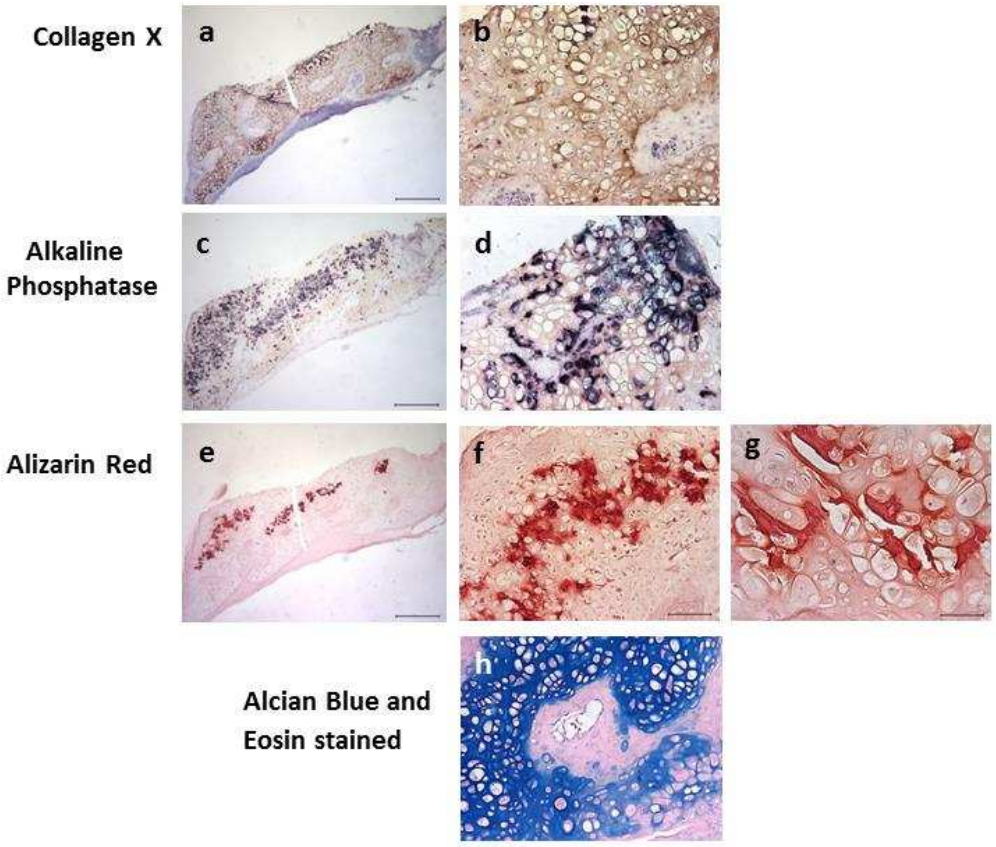

Figure 4: Representative histological and immunochemical sections of the retrieved constructs after 4 weeks of subcutaneous implantation. The images show distribution of collagen X **(a, b),** alkaline phosphatase (**c, d**), calcium deposition in Alizarin Red stained images **e** to **g**) and decreased staining for glycosaminoglycans from the areas invaded by blood vessels (Alcian Blue/Eosin stained section, **h**). Scale bars = 500 µm (**a, c, e)** 100 µm (**b**, **d**, **f**, **h**) and 50 µm (**g**).

In contrast, no mineralisation was observed in the constructs which were maintained in in vitro culture for an additional period of 4 weeks (Supplementary Figure 5) although extensive deposition of collagen X and alkaline phosphatase activity was observed during the extended culture period.

Cranial implantation

The pre-implantation constructs after 35 days of differentiation showed a hypertrophic phenotype in terms of large cell size, collagen X and alkaline phosphatase expression (Supplementary Figure 6).

In the absence of cells and some ECM formation, PGA has a very rapid rate of dissolution releasing acidic degradation products which had the possibility of causing an inflammatory reaction in a relatively confined area close to the surface of the brain [39]. Therefore, a cell-free PGA scaffold could not be implanted into the empty defect. Implantation of a tissue engineered hypertrophic cartilage graft promoted bone mineralised formation at all time points examined (Figures 5a, 5b, 5c). After 4 weeks the hypertrophic graft gave 15.15 % mineralisation within the defect compared to 7.06 % in the untreated defects. Histological analysis indicated the initiation of vascularisation within the graft as well as a decrease in

GAG around the invading blood vessels by 4 weeks). At 8 weeks a significant increase was observed in the percentage bone volume of the treated defects compared to the untreated defect (22.94 % and 7.07 % respectively) (Figures 5**b** and 5**d**). This is also supported by the morphological appearance of the bone-like tissue which has formed within the defect when analysed histologically (Figure 6 **a, b**). By week 12, micro-CT data showed that 38.48 % of the defect was mineralised (Figures 5**c**, **d**) compared to the untreated defect (7.56%) and further remodelling of the hypertrophic cartilage into bone was also observed histologically. Little bone formation was observed within the calvarial defects which had remained empty (i.e. they had not received a hypertrophic cartilage construct). In these a fibrous tissue had formed bridging the defect (Supplementary Figure 7).

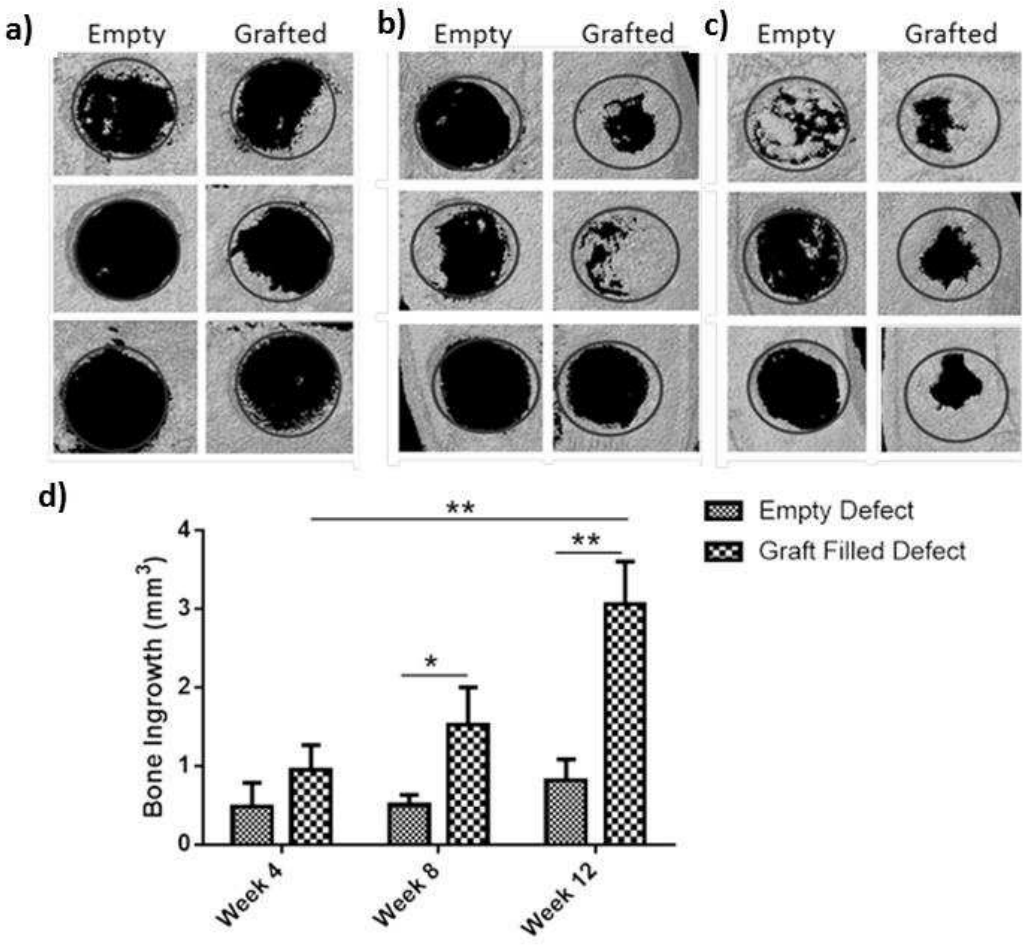

Figure 5: Micro-CT analysis of defects. (**a** – **c**) Micro-CT images showing the mineralisation within a 4 mm cranial defect either left empty with no graft material implanted or treated with a hypertrophic cartilage graft after implantation periods of **(a)** 4 weeks; (**b**) 8 weeks and (**c**) 12 weeks. Figure **5d** shows the volume of bone ingrowth determined by micro-CT within the defects throughout the healing period. (* $p<0.05$, ** $p<0.01$, n=3).

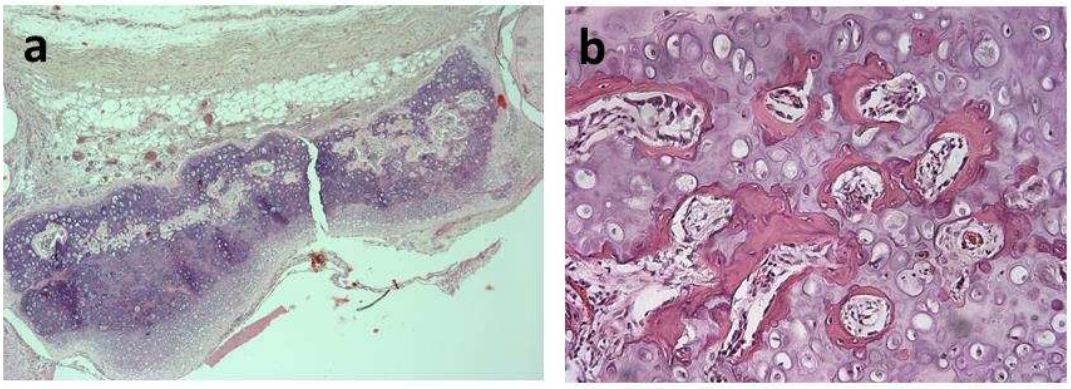

Figure 6: Representative images of the haematoxylin and eosin staining of decalcified sections of cranial defects treated with a hypertrophic cartilage graft after 8 weeks of in vivo implantation. Images show infiltration by blood vessels and formation of bone-like tissue around the areas of blood vessel infiltration. Total magnification: image (**a**) x40, image (**b**) x200.

4. Discussion

This is a proof of concept study using a rat model which shows the use of nasal chondrocytes to produce a tissue engineered hypertrophic construct in vitro. This study has demonstrated that this engineered hypertrophic cartilage material has the ability to undergo ossification and enhance bone regeneration in a bone defect in vivo. Non-woven PGA was chosen as a scaffold material as these polyesters have been well researched for tissue-engineering as they have Food and Drug Administration approval for clinical use [38]. PGA has the disadvantage of releasing glycolic acid by-products during degradation, and has been reported to induce inflammation and necrosis of nearby tissues [39]. Use of a PGA scaffold allowed for good cell attachment, proliferation and hypertrophic differentiation. On subcutaneous implantation of the hypertrophic constructs, a mild inflammatory response was observed on the periphery of the construct indicated by immunolocalisation of macrophages (CD 45+ cells) and lymphocytes (CD68+cells). No obvious inflammation was observed on implantation of the hypertrophic constructs into the cranial bone defect model.

The tissue engineered hypertrophic cartilage produced in this study was shown to have similar features to that seen in the growth plate. The engineered tissue exhibited a large cellular morphology and expressed the classical hypertrophic cartilage markers of collagen type X and alkaline phosphatase in the extracellular matrix. The temporal gene expression of Sox9, collagens II and X, Runx2 and alkaline phosphatase during the in vitro culture period in the nasal chondrocyte/PGA constructs also reflected that observed during chondrocyte hypertrophy within the growth plate [41]. Chondrocytes are well known to dedifferentiate during 2D culture conditions which are used to expand the numbers of cells for seeding onto scaffolds [40]. During 3D culture, the gene expression of collagen II was elevated by day 7 and indicative of the chondrocytes regaining a hyaline chondrogenic phenotype. By day 14

the collagen II gene expression was significantly down regulated and collagen X expression increased with alkaline phosphatase gene expression from day 7 of the culture reaching a peak at day 35 of culture. The temporal gene expression of signalling molecule, IHH, and transcription factors, Sox9 and Runx2 were also monitored throughout the differentiation period and found to reflect that reported for chondrocyte hypertrophy in the growth plate.

In the growth plate, IHH expression is localised to the area of post-mitotic, pre-hypertrophic chondrocytes which is adjacent to the proliferating columnar cells and regulates hypertrophic differentiation of chondrocytes [42]. IHH is reported to work through two mechanisms, inhibiting hypertrophic differentiation through the PTHrP pathway and Ptc-1 receptor or promoting hypertrophic differentiation through the Wnt/BMP pathway [42-45]. A peak of IHH gene expression was observed at day 21 just before a peak of Runx2 expression. Runx2 is essential during hypertrophic differentiation as it is known to regulate the expression of other genes associated with mineralisation and angiogenesis, including BMPs and VEGF to induce angiogenesis in the cartilage. Runx2 also promotes the extracellular matrix remodelling via synthesis of matrix metalloproteinases (MMPs) and osteopontin which enables osteoclast attachment [48-52]. These downstream proteins are essential for the subsequent mineralisation and bone formation within the tissue-engineered hypertrophic cartilage. Sox9 is believed to work via the PTHrP pathway to maintain cells in a proliferative state. [46]. Dy et al, however, have shown that Sox9 is also an important transcription factor for hypertrophic differentiation, where it is located to the nuclei of chondrocytes where it acts upon the collagen type X promoter both independently and through cooperation with mef2c [47]. We observed downregulation of Sox9 throughout the culture period with increased Sox9 expression on day 35 which corresponded to the peak expression of collagen type X within the constructs.

This ability to create an engineered tissue with the morphological and phenotypical feature of natural hypertrophic cartilage is essential to allow of mineralisation and bone remodelling in vivo. While the production of an engineered tissue with characteristics of hypertrophic cartilage was successful in vitro on the PGA scaffold material, these constructs failed to show cartilage mineralisation in vitro. However, the constructs did undergo cartilage mineralisation on in vivo implantation (Figure 4) but not on extended in vitro culture. Mineralisation of hypertrophic cartilage is a prerequisite step for the later ossification. There are several hypotheses as to why cartilage mineralisation did not occur in vitro. Either the culture conditions used were not conducive to cartilage mineralisation by the hypertrophic chondrocytes or that the interaction of another cell type, for example, endothelial or osteoblast progenitors, was required in order for initiation of the cartilage mineralisation stage.

On in vivo subcutaneous implantation vascularisation of the tissue constructs occurred before subsequent mineralisation and bone formation was observed. Endothelial progenitors and haematopoietic stem cells which express $CD34^{+}$ have previously been shown to be important for the neovascularisation of fractures and subsequent fracture healing [53]. Olmsted-Davis et al observed that CD34+ cells have the ability to generate osteogenic cells, which can express osteogenic markers, osteocalcin and alkaline phosphatase [54]. The decrease in ECM observed around the vascularisation of the graft can be attributed to the vascularisation of the hypertrophic cartilage. MMPs have been shown to be expressed by and around areas of vascularisation, including MMP-9 (gelatinase B) which has been shown to degrade collagens within the ECM of hypertrophic cartilage [55]. This need for the initial vascularisation of the tissue constructs highlights the importance of the expression of angiogenic factors, such as VEGF, within the grafts in order to recruit the CD34+ cells [11].

On implantation into a cranial bone defect, the nasal chondrocyte/PGA constructs were invaded by blood vessels and the cartilage was re-modelled into bone-like tissue. Although the size of bone defect used enabled self-healing given sufficient time; the bone defects containing the nasal chondrocyte/PGA constructs showed significantly more bone regeneration. The bone regeneration observed within the hypertrophic cartilage grafts after in vivo implantation therefore may be a downstream reaction to the invasion of the tissue by blood vessels and the degradation of the hypertrophic cartilage matrix, as vascularisation allows for the influx of osteoblasts and monocyte-derived osteoclasts to regulate bone formation [12].

5. Conclusion

There are relatively few studies looking at the potential of using hypertrohic cartilage as a potential method to produce a bone graft substitute and most of this research is directed to using bone marrow derived MSCs to engineer cartilage constructs with hypertrophic cartilage features. This study shows that that adult nasal chondrocytes can be used to produce a tissue engineered hypertrophic cartilage-like tissue with morphological and phenotypical similarities to that of the hypertrophic cartilage found within a growth plate. Furthermore, this engineered hypertrophic cartilage can undergo vascularisation and enable subsequent bone formation once implanted in vivo, in a bone defect. Within the 14 months there has been a single report showing that hypertrophic cartilage grafts formed from nasal chondrocytes (adult human nasal chondrocytes) could undergo endochondral ossification in a nude mouse (Pippenger et al, [30]). The use of nasal chondrocytes to produce a hypertrophic cartilage is an exciting progression in developmental engineering and further research into this area has potential to lead to the production of a new clinical bone graft substitute for bone grafting.

Acknowledgements

The authors would like to acknowledge the European commission (Marie Curie Alea Jacta EST, contract MEST-CT-2004-008104) University of Sheffield for funding this research.

References

[1] Gupte MJ, Ma PX. Nanofibrous Scaffolds for Dental and Craniofacial Applications. J Dental Res. 2012;91:227-34.

[2] Goulet JA, Senunas LE, DeSilva GL, Greenfield M. Autogenous iliac crest bone graft - Complications and functional assessment. Clin Orthopaedics and Related Res. 1997:76-81.

[3] Zhao JJ, Griffin M, Cai J, Li SX, Bulter PEM, Kalaskar DM. Bioreactors for tissue engineering: An update. Biochemical Engineering Journal. 2016;109:268-281.

[4] Mabvuure N, Hindocha S, Khan WS. The Role of Bioreactors in cartilage tissue engineering Cur Stem Cell Res & Ther. 2012;7(4):287-292.

[5] Kirkpatrick CJ, Fuchs S, Unger RE. Co-culture systems for vascularization - Learning from nature. Advan Drug Deliv Rev 2011; 63 (4-5) Special Issue SI:291-299.

[6] Wuelling M, Vortkamp A. Transcriptional networks controlling chondrocyte proliferation and differentiation during endochondral ossification. Ped Nephrology 2010;25:625-31.

[7] Scotti C, Tonnarelli B, Papadimitropoulos A, Scherberich A, Schaeren S, Schauerte A, et al. Recapitulation of endochondral bone formation using human adult mesenchymal stem cells as a paradigm for developmental engineering. Proc Natl Acad Sci USA. 2010;107:7251-6.

[8] Gawlitta D, Farrell E, Malda J, Creemers LB, Alblas J, Dhert WJA. Modulating endochondral ossification of multipotent stromal cells for bone regeneration. Tissue Eng Part B Rev. 2010;16:385-95.

[9] Hirao M, Tamai N, Tsumaki N, Yoshikawa H, Myoui A. Oxygen tension regulates chondrocyte differentiation and function during endochondral ossification. J Biol Che. 2006;281:31079-92.

[10] Inada M, Wang YM, Byrne MH, Rahman MU, Miyaura C, Lopez-Otin C, et al. Critical roles for collagenase-3 (Mmp13) in development of growth and in endochondral plate cartilage ossification. Proc Nat Acad Sciences of the USA. 2004;101.

[11] Ortega N, Wang K, Ferrara N, Werb Z, Vu TH Gerber HP, Vu TH, Ryan AM, Kowalski J, Werb Z, Ferrara N. Complementary interplay between matrix metalloproteinase-9, vascular endothelial growth factor and osteoclast function drives endochondral bone formation. Disease Models & Mechanisms. 2010; 3(3-4):224-23.

[12] Gerber HP, Ferrara N. Angiogenesis and bone growth. Trends in Cardiovascular Medicine. 2000;10:223-8.

[13] Sato M, Morii E, Komori T, Kawahata H, Sugimoto M, Terai K, et al. Transcriptional regulation of osteopontin gene in vivo by PEBP2 alpha A/CBFA1 and ETS1 in the skeletal tissues. Oncogene. 1998;17:1517-25.

[14]Vinatier C, Guicheux J. Cartilage tissue engineering: From biomaterials and stem cells to osteoarthritis treatments. Ann Physical and Rehab Medicine. 2016;59:139-144.

[15] Nazempour A, Van Wie BJ. Chondrocytes, mesenchymal stem cells and their combination in articular cartilage regenerative medicine. Ann of Biomed Eng. 2016;44(5):1325-1354.

[16] Pleumeekers MM, Nimesskern L, Koevoet WLM, Karperien M, Stok KS, van Osch GJVM. Cartilage regeneration in the head and neck area: Combination of ear or nasal

chondrocytes and mesenchymal stem cells improves cartilage production. Plastic and Reconstructive Surg. 2015;136(6):762E-774E.

[17] Fulco I, Miot S, Haug MD, Barbero A, Wixmerten A, Feliciano S et al. Engineered autologous cartilage tissue for nasal reconstruction after tumour resection\; an observational first-in-human trial. Lancet. 2014;384(9940):337-346.

[18] Oseni A, Crowley C, Lowdell M, Birchall M, Butler PE, Seifalian AM.Advancing nasal reconstructive surgery: the application of tissue engineering technology. Journal of Tiss Eng and Regen Med. 2012;6(10):757-768.

[19] Scotti C, Piccinini E, Takizawa H, Toderov A, Bourgine P, Papadimitropoulos A. et al. Engineering of a functional bone organ through endochondral ossification. Proc Nat Acad Sci. 2013;110(10):3997-4002.

[20] Sheey EJ, Mesallati T, Kelly L, Vinardell T, BuckleyCT, Kelly DJ. Tissue engineering whole bones through endochondral ossification: Regenerating the distal phalanx. Bioresearch Open Access.2015;4(1):229-241.

[21] Wei X, Yang X, Han Z, Qu F, Shao L, Shi Y. Mesenchymal stem cells: a new trend for cell therapy. Acta Pharmacologica Sinica. 2013;34:747-54.

[22] Bernstein P, Sticht C, Jacobi A, Liebers C, Manthey S, Stiehler M. Expression pattern differences between osteoarthritic chondrocytes and mesenchymal stem cells during chondrogenic differentiation. Osteoarthritis & Cartilage.2010;18:1596-607.

[23]Pelttari K, Steck E, Richter W. The use of mesenchymal stem cells for chondrogenesis. Injury-Int Journal Care of the Injured. 2008;39:S58-S65.

[24] Kafienah W, Jakob M, Demarteau O, Frazer A, Barker M, Martin I, et al. Three-dimensional tissue engineering of hyaline cartilage: Comparison of adult nasal and articular chondrocytes. Tissue Engineering. 2002;8:817-26.

[25] Stringer B, Waddington R, Sloan A, Phillips I, Telford G, Hughes D, et al. Bespoke human hypertrophic chondrocytic cell lines provide the osteoinductive signals required for vascularized bone formation. Tissue Engineering. 2007;13:133-45.

[26] Oyajobi BO, Frazer A, Hollander AP, Graveley RM, Xu C, Houghton A, et al. Expression of type X collagen and matrix calcification in three-dimensional cultures of immortalized temperature sensitive chondrocytes derived from adult human articular cartilage. J Bone and Mineral Res.1998;13:432-42.

[27] Gharravi AM, Orazizadeh M, Hashemitabar M. Fluid-induced shear improves cartilage-like tissue fabrication by encapsulating chondrocytes. Cell and Tissue Banking. 2016;17(1):117-122.

[28] Barandum M, Iselin LD, Santini F, Pansini M, Scotti C, Baumhoer D. et al. Generation and characterisation of osteochondral grafts with human nasal chondrocytes. J Ortho Res. 2015; 33(8): 1111-1119.

[29] Bermueller C, Schwarz S, Elsaesser AF, Sewing J, Baur N, von Bomhard A. et al. Marine collagen scaffolds for nasal cartilage repair: Prevention of nasal septal perforations in a new orthotopic rat model using tissue engineering techniques. Tissue Engineering Part A. 2013; 19 (19-20):2201-2214.

[30] Pippenger BE, Ventura M, Pelttari K, Feliciano S, Jaquiery C, Scherberich A. et al. Bone forming capacity of adult human nasal chondrocytes. J Cell Mol Med. 2015;19(6):1390-1399.

[31] Elsaesser AF, Schwartz S, Joos H, Koerber L, Brenner RE, Rotter N. Characterisation of a migrative subpopulation of adult human nasoseptal chondrocytes with progenitor cell features and their potential for in vivo cartilage regeneration studies. Cell & Bioscience. 2016;6(11): DOI 10.1186/s13578-016-0078-6.

[32] Crawford A, Dickinson SC. Chondrocyte isolation, expansion and culture on polymer scaffolds: Methods in Molecular Biology 238:147-158. Humana Press Inc; 2004

[33] Olivera SM, Amaral, IF, Barbosa MA, Teixeira CC. Engineering endochondral bone: In vitro studies. Tissue Engineering Part A. 2009;15(3):625-634.

[34] De Maria C, Giusti S, Mazzei D, Crawford A, Ahluwalia. Squeeze Pressure Bioreactor: A Hydrodynamic Bioreactor for Noncontact Stimulation of Cartilage Constructs. Tissue Engineering Part C. 17;(7):757-763.

[35] Madry H, Kaul G, Zurakowski D, Vunjak-Novakovic G, Cucchiarini M. European Cells & Materials.2013; 25: 229–247.

[36] Tare RS, Howard D, Pound JC, Roach HI, Oreffo ROC. Tissue engineering strategies for cartilage generation. Micromass and three dimensional cultures using human chondrocytes and a continuous cell line. Biochim Biophys Res Commun. 2005;333(2):609-621.

[37] Farndale RW, Buttle DJ, Barrett AJ. Improved quatitation and discrimination of sulphated glycosaminoglycans by use of dimethylmethylene blue. Biochim Et Biophys Acta. 1986;883:173-7.

[38] Ueda H, Tabata Y. Polyhydroxyalkanonate derivatives in current clinical applications and trials. Advan Drug Delivery Rev. 2003;55:501-18.

[39] Shoichet MS. Polymer Scaffolds for Biomaterials Applications.. Macromolecules. 2010;43:581-91.

[40] Caron MM, Emans PJ, Coolsen MM, Voss L, Surtel DA, Cremers A, et al. Redifferentiation of dedifferentiated human articular chondrocytes: comparison of 2D and 3D cultures. Osteoarthritis & Cartilage. 2012;20:1170-8.

[41] Wardale RJ, Duance VC. Characterisation of articular and growth plate cartilage collagens in porcine osteochondrosis. J Cell Sci. 1994;107 (Pt 1):47-59.

[42] Mak KK, Kronenberg HM, Chuang PT, Mackem S, Yang YZ. Indian hedgehog signals independently of PTHrP to promote chondrocyte hypertrophy. Development. 2008;135:1947-56.

[43] Pateder DB, Rosier RN, Schwarz EM, Reynolds PR, Puzas JE, D'Souza M, et al. PTHrP expression in chondrocytes, regulation by TGF-beta, and interactions between epiphyseal and growth plate chondrocytes. Exp Cell Res. 2000;256.

[44] Lai LP, Mitchell J. Indian hedgehog: Its roles and regulation in endochondral bone development. J Cell Biochem. 2005;96:1163-73.

[45] St-Jacques B, Hammerschmidt M, McMahon AP. Indian hedgehog signaling regulates proliferation and differentiation of chondrocytes and is essential for bone formation. Genes & Development. 1999;13:2072-86.

[46] Hattori T, Muller C, Gebhard S, Bauer E, Pausch F, Schlund B, et al. SOX9 is a major negative regulator of cartilage vascularization, bone marrow formation and endochondral ossification. Development. 2010;137:901-11.

[47] Dy P, Wang W, Bhattaram P, Wang Q, Wang L, Ballock RT, et al. Sox9 Directs Hypertrophic Maturation and Blocks Osteoblast Differentiation of Growth Plate Chondrocytes. Developmental Cell. 2012;22:597-609.

[48] Kim IS, Otto F, Zabel B, Mundlos S. Regulation of chondrocyte differentiation by Cbfa1. Mechanisms of Development. 1999;80:159-70.

[49] Zelzer E, Glotzer DJ, Hartmann C, Thomas D, Fukai N, Soker S, et al. Tissue specific regulation of VEGF expression during bone development requires Cbfa1/Runx2. Mechanisms of Development. 2001;106:97-106.

[50] Provot S, Schipani E. Molecular mechanisms of endochondral bone development. B Reinholt FP, Hultenby K, Oldberg A, Heinegard D. Osteopontin - A possible anchor of osteoclasts to bone. Proc Natl Acad Sci USA. 1990;87:4473-5.

[51] Komori T. Regulation of skeletal development by the Runx family of transcription factors. J Cell Biochem. 2005;95:445-53.

[52] Matsumoto T, Kuroda R, Mifune Y, Kawamoto A, Shoji T, Miwa M, et al. Circulating endothelial/skeletal progenitor cells for bone regeneration and healing. Bone.2008;43:434-9.

[53] Olmsted-Davis EA, Gugala Z, Camargo F, Gannon FH, Jackson K, Kienstra KA, et al. Primitive adult hematopoiletic stem cells can function as osteoblast precursors. Proc Natl Acad Sci USA.
2003;100:15877-82.

[54] Vu TH, Shipley JM, Bergers G, Berger JE, Helms JA, Hanahan D, et al. MMP-9/gelatinase B is a key regulator of growth plate angiogenesis and apoptosis of hypertrophic chondrocytes. Cell.1998;93:411-22.

Supplementary Data

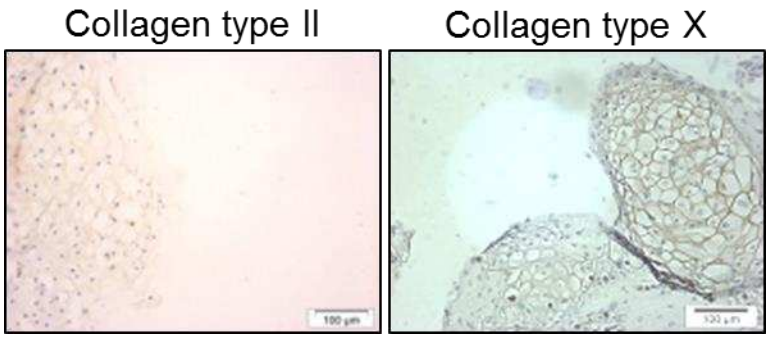

Supplementary Figure 1: Representative immunohistochemical controls for immunolocalisation of collagen type II and collagen type X (scale bars 100 µm)

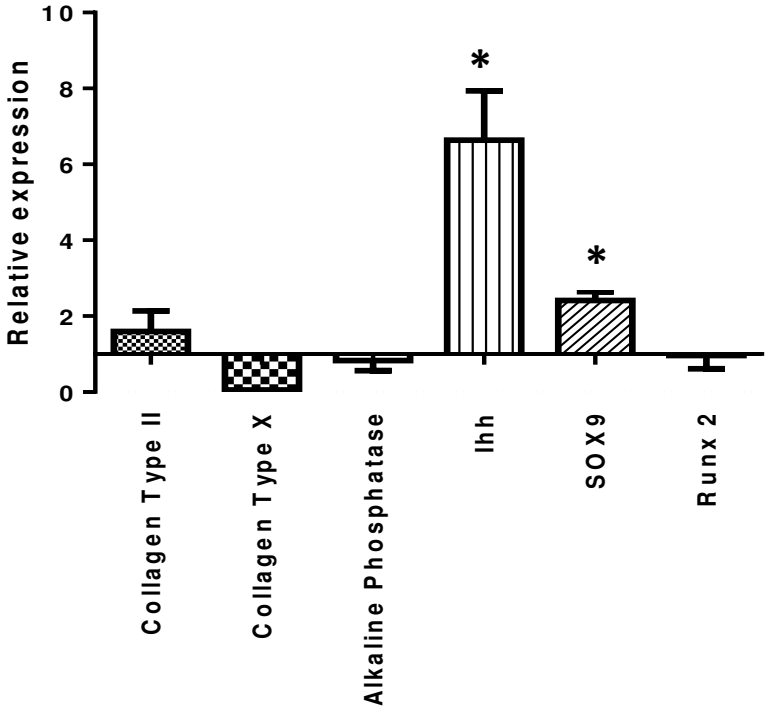

Supplementary Figure 2: Effect of 3D culture on the gene expression of chondrocytes relative to the expression profile observed in chondrocytes maintained in a 2D tissue culture environment. Collagen type II, collagen type X, alkaline phosphatase, Ihh, Sox9 and Runx2

expression within the chondrocytes were all assessed after the 72h scaffold seeding period (n=3, *p=0.05).

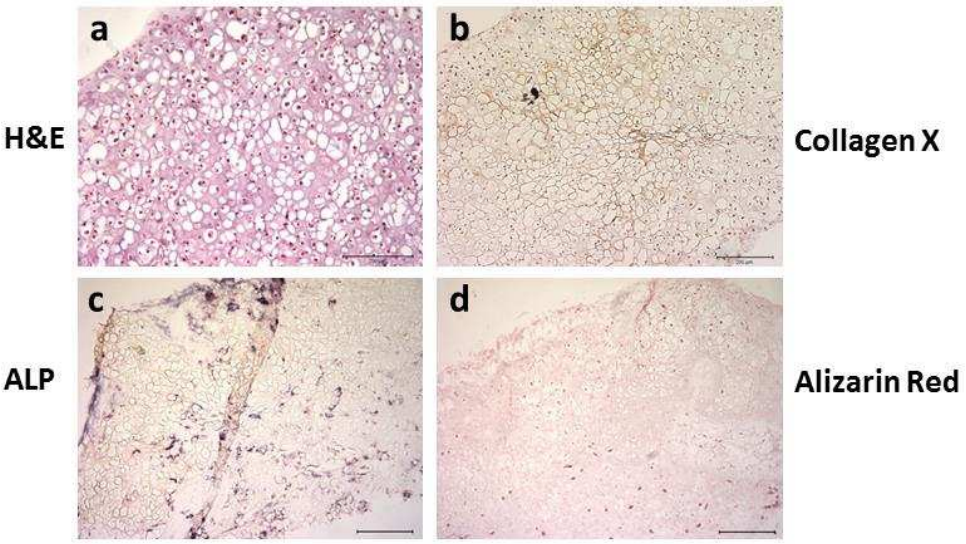

Supplementary Figure 3: Histological and immunohistochemical images of tissue sections of the nasal chondrocyte/PGA constructs after 42 days in vitro culture and prior to subcutaneous implantation. Images show the general tissue morphology (H&E stained section, **a**) collagen X deposition (**b),** alkaline phosphatase activity, ALP (**c)** and lack of mineralisation as detected by Alizarin Red staining (d). Scale bars =200 µm.

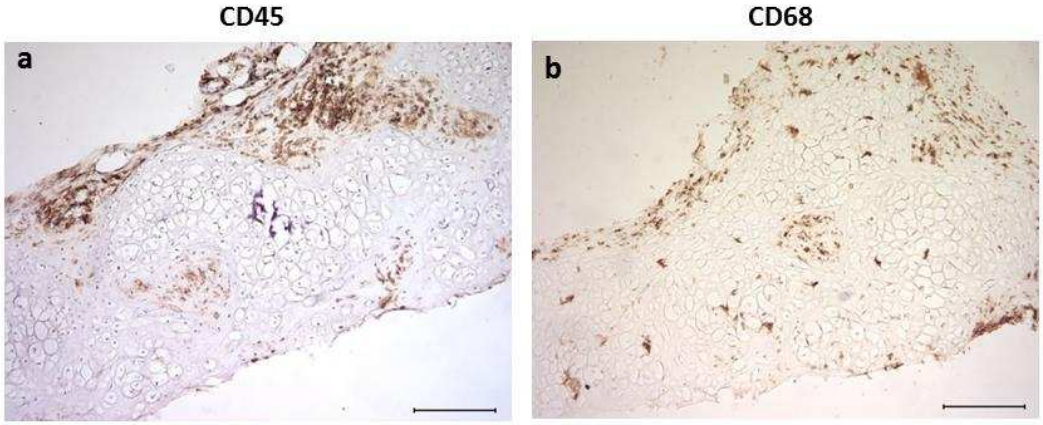

Supplementary Figure 4: Representative images of tissue sections showing immunolocalisation of CD45 (**a**) and CD68 (**b**) taken from nasal chondrocyte constructs 4 weeks after subcutaneous implantation. The images indicate a moderate level of leucocyte (CD45+ve) and macrophage (CD68+ve) infiltration on the periphery of the construct, around blood vessels with little infiltration in the body of the tissue.

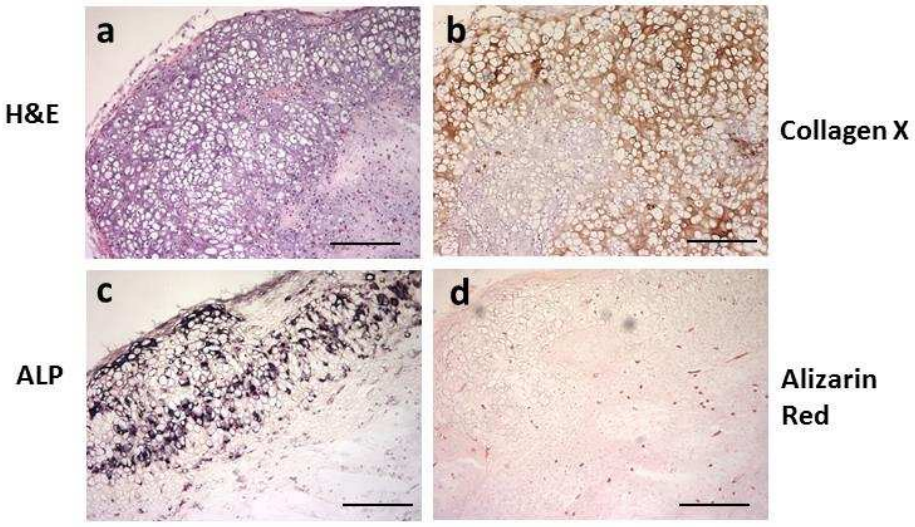

Supplementary Figure 5: Representative images of tissue sections nasal chondrocyte/PGA constructs after 8 weeks in in vitro culture. Images show the general tissue morphology (H&E stained section, **a**) collagen X deposition (**b**), alkaline phosphatase activity, ALP (**c**) and lack of mineralisation as detected by Alizarin Red staining (d). Scale bars= 200 µm.

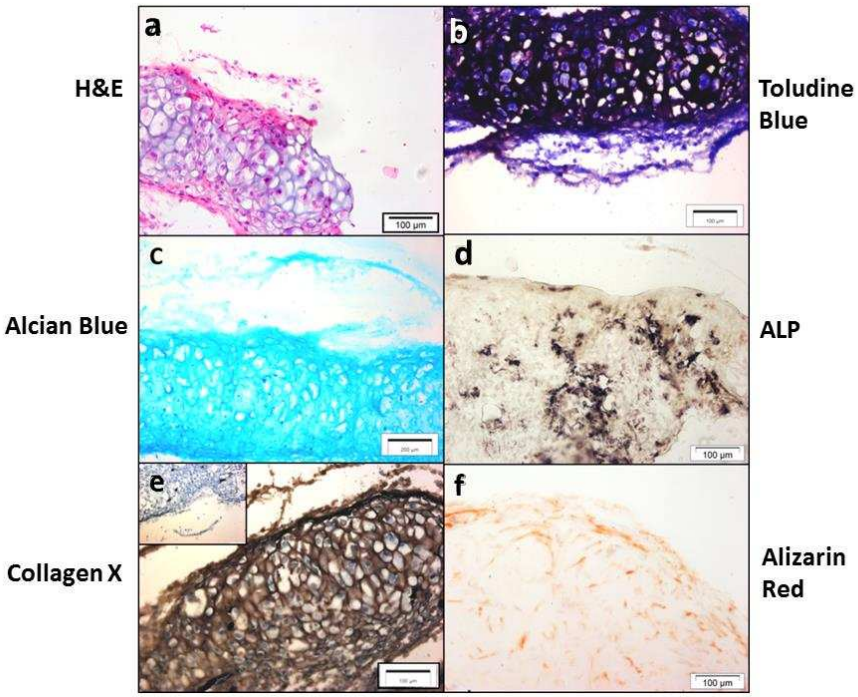

Supplementary Figure 6: Histological and immunohistochemical images of tissue sections of the nasal chondrocyte/PGA constructs after 35 days in vitro culture and prior to implantation in a calvarial cranial defect. The images show typical features of hypertrophic chondrocytes. The general tissue morphology showed increased cell volume [H&E stained section (**a**)] and proteoglycan deposition [purple coloured areas in Toluidine Blue-stained section (**b)** and light blue colour in Alcian Blue stained section (**d)**].The constructs also showed of collagen X deposition [brown stained areas, in image (**e**)]. The inset image in (**e**) shows the non-specific binding control. Alkaline phosphatase activity (ALP) was observed (black staining in image (**d**) and lack of mineralisation was observed as detected by Alizarin Red staining (**f**). Scale bars =200 µm.

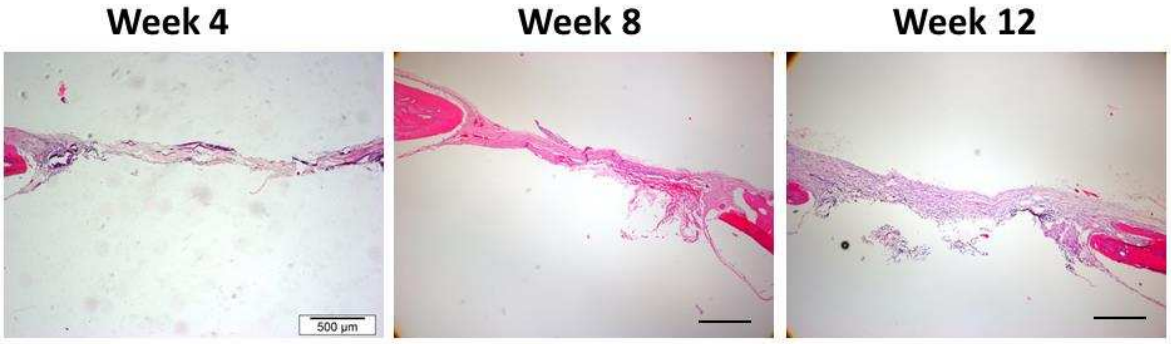

Supplementary Figure 7: Representative images of tissue sections of the empty calvarial defects (no nasal chondrocyte-PGA hypertrophic construct implanted).The images show H&E stained sections taken from calvaria 4, 8 and 12 weeks after the defects were surgically created. Formation of a fibrous strand of tissue bridging the defects was observed with some bone regeneration occurring around the edge of the defect. However, no bone formation was seen towards the centre. (n=3 per time point). Scale bars= 500 µm.